Received: Added at production | Revised: Added at production | Accepted: Added at production

DOI: xxx/xxxx

ARTICLE TYPE

Time and Phase Alignment of Distributed Gateways: Theoretical Analysis and Experimental Demonstration

Eriserdi Mollaymeri* | Thomas Delamotte | Andreas Knopp

Institute of Information Technology, University of the Bundeswehr Munich, Bavaria, Germany

Correspondence
*Eriserdi Mollaymeri
Email: papers.sp@unibw.de

Present Address
Institute of Information Technology, University of the Bundeswehr Munich, Werner-Heisenberg-Weg 39, D-85579 Neubiberg, Germany

Summary

Very high throughput satellite systems have recently been developed to offer high-speed connectivity, especially in remote areas, planes and ships. The high data rates can be achieved by using a multibeam approach with an aggressive reuse of the available frequency resources. Due to the high number of user beams, the system must support a large aggregated bandwidth. Multiple-gateway architectures are a necessary solution to sustain the immense bandwidth requirements. Multiple-input multiple-output (MIMO) feeder links have been proposed to address the ground segment design challenges of multiple-gateway architectures. The deployment costs and the link availability performance can in particular benefit from this approach. However, to coordinate the operation of multiple gateways, high precision time and phase synchronization is necessary. In this paper, the effect of time and phase misalignment in NxN MIMO feeder links is studied. The performance limitation due to imperfect time and phase distribution is analyzed. Synchronization via optical fiber is considered in this study. The accuracy of time distribution was verified through laboratory measurements. The impact of the residual timing error on the achievable system bandwidth was assessed. Results showed that several GHz of bandwidth can be supported. On the other hand, a recently proposed phase synchronization approach is considered as a promising candidate for MIMO feeder links. Its phase stability performance is assessed and it is emphasized that requirements in terms of link outage are fulfilled.

KEYWORDS:
HTS systems, Multiple-gateway systems, MIMO feeder link, Time synchronization, Phase synchronization.

1 | INTRODUCTION

High throughput satellite (HTS) systems are at the forefront of advancements for satellite communications, allowing for capacities of over 1 Tb/s [1]. Unlike classical satellite applications, HTS systems are based on frequency reuse and geographically separated user beams [2]. This allows for the beams to cover smaller regions, instead of serving areas as big as continents. However, serving multiple user beams at the same time is a demanding task. Furthermore, because computing resources on-board the satellites are limited, most of the signal processing applied in the forward link are performed at the transmitter side, i.e. in the gateways.

Different downlink optimization techniques have been adopted in HTS systems to cope with the high data traffic demands. One such solution is aggressive frequency reuse in the user links. Precoding is implemented to mitigate the interference between the user beams of these architectures. The interference of beams within the same cluster and in different clusters has been thoroughly studied and precoding methods to reduce it have been designed [3,4]. Moreover, distributed predistortion techniques are proposed to improve the spectral and power efficiency in non-linear

satellite channels[5]. Performance optimization algorithms for the non-orthogonal multiple-access (NOMA) beamforming architectures have also been investigated[6]. These algorithms facilitate serving multiple users per beam in the same time slot. Furthermore, beam-hopping techniques are considered for a more efficient allocation of the available resources according to the traffic demands, even among different clusters of beams[7,8]. Another acknowledged approach is employing digital transparent payloads for HTS systems[9]. The main motivation of digital transparent payloads is to enable a flexible allocation of the physical layer resources on-board the satellite.

Proper dimensioning of the feeder links for the HTS systems is also a requirement to support the higher data rate. Due to the limited uplink frequency resources, single gateway systems are not able to support the increased traffic, even if higher frequency bands like Q/V (5 GHz available) or even W band (also 5 GHz available) are used. As a consequence, a large number of ground stations separated by hundreds of kilometers from each other must be deployed. The development of such systems is a burdensome and costly task. Recent works proposed multiple-input multiple-output (MIMO) feeder links as a candidate to overcome several implementation bottlenecks that multiple-gateway architectures face[10,11]. MIMO systems consist on using multiple transmit and receive antennas operating simultaneously by exploiting spatial multiplexing. MIMO feeder links could contribute to the cost reduction of the ground segment, allow for a more efficient placement of the ground stations and improve the performance under atmospheric perturbations. While other applications consider the implementation of MIMO precoding to mitigate interference between spatially separated feeder links[12], the approach of MIMO feeder links consists on using precoding to enable spatial multiplexing from ground stations located in the same beams.

However, the ground-based processing techniques in multiple-gateway systems require high precision coordination between the gateways for a successful operation. For example, in the case of precoding, it is necessary to have the gateways synchronized in time and phase[12]. In another application, it is demonstrated that while dealing with predistortion in multiple-gateway systems, a deviation of the baseband signals from the ideal case due to a drift in time or phase causes the system to undergo a significant performance loss[5]. Phase and time synchronization is a practical aspect that is only rarely considered in theoretical studies. Nevertheless, synchronization in such distributed systems remains a troublesome task as the desire for higher capacity necessitates always better performing alignment. In this paper, we address the time and phase misalignment problem in multiple-gateway architectures that employ the MIMO feeder link technique.

As with MIMO feeder links and multiple-gateway architectures in general, highly stable distribution of time and frequency over long distances is a necessity in many other applications. Among a few time dissemination techniques, the most predominant are satellite-based schemes, such as the Global Positioning System (GPS)[13,14]. Albeit popular and easy to access, these systems are becoming obsolete over time due to their limited ability for stable distribution, with typical uncertainty values of 10 ns to 20 ns[15,16,17]. The increasing demand for higher precision requires other approaches. Radio signals in the VHF (144-148 MHz) and UHF (420-450 MHz) amateur frequency bands have been proposed for aligning handheld ground receivers separated by a few kilometers[18]. However, the MIMO feeder link approach requires the ground stations to be tens of kilometers away. In the recent years, distribution of time and frequency over optical fiber has been intensively studied as a candidate solution. Compared to satellite-based techniques, fiber links are less prone to external perturbations and they guarantee broad bandwidth, low attenuation and scalability. Experiments prove that sub-nanosecond time misalignment values can be maintained over long distances[19]. Furthermore, the optical fiber time distribution approach has already found practical application[20].

Likewise, due to the aforementioned characteristics, optical fiber is also the preferred solution for stable frequency distribution to ground stations separated by long distances[20]. Another advantage is that, transmission over fiber suffers from relatively low phase noise[21]. Using fiber for both time and frequency distribution is also a cost effective solution because synchronization can be implemented on the existing fiber infrastructure used for data transfer[22]. In general, the methods for phase synchronization through stable frequency distribution over fiber are separated in two major techniques: active phase compensation and passive phase compensation[23]. Passive compensation is an open-loop scheme, which is based on frequency mixing to cancel out the phase noise accumulated during transmission over the fiber[23,24]. On the other hand, active compensation employs a feedback loop (closed-loop) to compensate for the phase noise with the help of voltage-controlled or digitally-controlled oscillators[20,21,22]. The passive compensation technique is still in its infancy and its performance is strikingly dependent on the quality of the mixers being used[24]. As a result, the active compensation technique continues to be the most favored solution and has already been practically tested[22].

We focus in this work on the impact of time and phase misalignment between the ground antennas in an NxN MIMO feeder link with a Geostationary Earth Orbit (GEO) satellite. Mathematical models that describe the performance limitation due to imperfect time and phase distribution were developed. An experiment was implemented to test the ability of the optical fiber for high precision time synchronization. For the experiment, we synchronized in time two White Rabbit devices, which are a commercially available solution for optical fiber time distribution. The White Rabbit devices were connected with a few tens of kilometers long fiber. The experimental results were used as input to our transmission chain model and the impact of the imperfections on the performance was evaluated. Regarding phase synchronization, the results from an already experimentally tested technique for the Square Kilometre Array project[22] are exploited. The phase uncertainty numbers measured in this application were applied to our mathematical model and the performance penalty on the carrier to interference plus noise ratio (CINR) was evaluated.

The rest of the paper is organized as follows. In Section 2, the system architecture for an NxN MIMO feeder link is introduced. Furthermore, time and phase impairments affecting this setup are analyzed. The impact of the residual time and phase misalignment due to imperfect synchronization

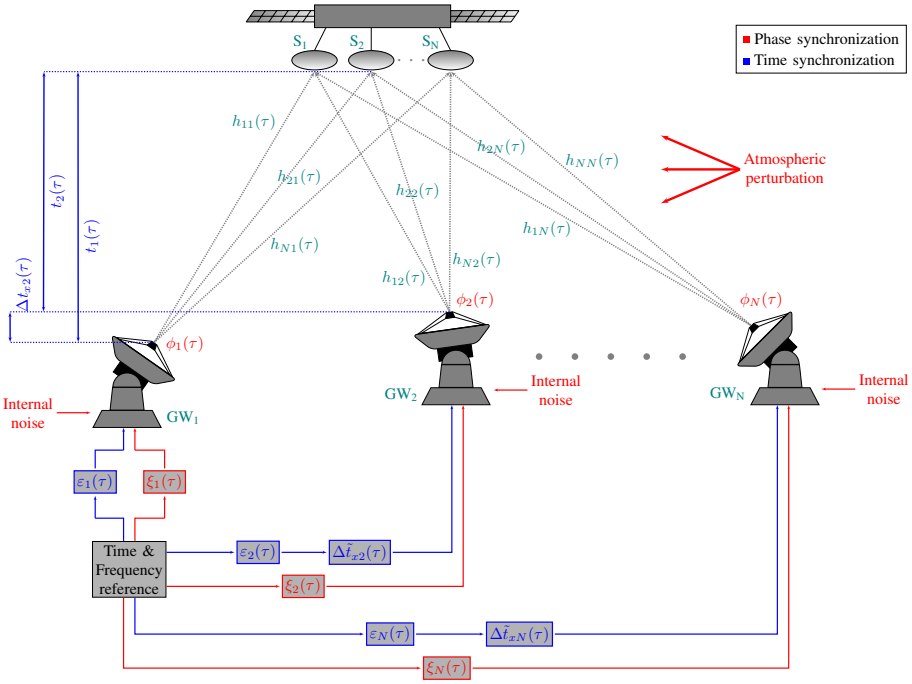

Figure 1 NxN MIMO feeder link with time and phase impairments.

on the performance of an NxN MIMO feeder link is explained in Sections 3 and 4 accordingly. In Section 5, the experiment for time synchronization of two White Rabbit devices over a few tens of kilometers long optical fiber is demonstrated. Additionally, the concept behind the phase synchronization technique implemented in the Square Kilometre Array project is explained. The numerical results are compared with the analysis of Sections 3 and 4 to assess the practical feasibility of MIMO feeder links using the proposed synchronization solutions. Lastly, conclusions are drawn in Section 6.

2 | SYSTEM ARCHITECTURE

The architecture of an NxN MIMO feeder link is illustrated in Fig. 1. The ground stations transmit to a GEO satellite, which uses multiple antennas to receive the signals. $h_{mn}(\tau)$ represents the coefficient for the channel between the m-th satellite antenna and the n-th ground antenna. τ is used to indicate the observation time instant. Even though it is not the focus of this work, a proper implementation of the MIMO feeder link involves precoding of the signal streams at the ground stations [10]. The performance of the MIMO feeder link is particularly dependent on the phase and time alignment between the transmission paths to the satellite. This section analyzes this dependency and introduces the sources of imperfections. In Fig. 1, the blue color is used to indicate the components and variables related to time synchronization. On the other hand, with the red color are marked the components and variables related to phase synchronization.

Unlike for the forward feeder link, time and phase synchronization of the ground stations is unnecessary for the return link. MIMO post-processing can compensate the time and phase downlink uncertainties at the ground receivers. This can be done with the help of pilot symbols [11]. Therefore, the return link is not considered in Fig. 1 and for the remainder of the paper.

2.1 | Time impairments

For the sake of simplicity, in Fig. 1, we concentrate on the two gateways on the left (referred to as GW_1 and GW_2 in the following) and the twomai satellite antennas on the left (referred to as S_1 and S_2 in the following). $t_1(\tau)$ in Fig. 1 represents the propagation time from GW_1 to the satellite. Similarly, $t_2(\tau)$ represents the propagation time from GW_2 to the satellite. The path lengths can strongly differ due to the large separation between the ground antennas. Additionally, even though the satellite position is expected to be fixed with respect to an observer on Earth, the path lengths vary slowly over time due to the satellite's movement in its station keeping box. As a consequence, there is an always changing difference in transmission times between the ground antennas and the satellite. This time perturbation is illustrated with $\Delta t_{x2}(\tau) = t_1(\tau) - t_2(\tau)$ in the figure.

In an ideal scenario, the parameter $\Delta t_{x2}(\tau)$ is the only timing mismatch between the transmission paths of the two ground antennas. The available literature has already provided mathematical models to study its behavior [10,25]. Furthermore, it has been shown that, as long as the satellite movement is continuously tracked, it is possible to compensate the time difference between the uplink paths [26]. This can be done by introducing a controlled delay to GW_2, namely $\Delta\tilde{t}_{x2}(\tau)$ in Fig. 1 [27]. Ideally, the delay introduced at GW_2 must be equal to $\Delta t_{x2}(\tau)$, because then it is guaranteed that the signals transmitted from GW_1 and GW_2 arrive exactly at the same time at the satellite. The same logic is applied for the rest of the gateways, where, at each gateway, a controlled delay is introduced so that the time differences with GW_1 are cancelled out.

If the ground antennas are not synchronized, the equality between the propagation time differences and the controlled delays cannot be guaranteed. As a consequence, a time synchronization technique should be applied to align the stations so that the signals can arrive at the same time at the satellite. To this end, a time reference block is added in Fig. 1. Once connected to the ground stations, it should distribute the time reference to them. Thus, the ground stations will be synchronized and the signals will arrive at the same time at the satellite. However, there will always be a residual time alignment error that varies over time. The time reference block is connected via fiber links to the ground stations, which might be placed tens of kilometers away. The distribution of the time reference over long distances can lead to imperfections of the time alignment. These impairments are mainly present due to hardware imperfections and temperature changes. Therefore, timing alignment mismatches $\varepsilon_1(\tau)$, $\varepsilon_2(\tau)$, ... and $\varepsilon_N(\tau)$, between the different ground stations and the reference source, are added in Fig. 1. In Section 3, the impact of the residual time misalignment and the minimum level of time synchronization accuracy for a MIMO feeder link are characterized.

2.2 | Phase impairments

For the MIMO feeder link in Fig. 1, the contributors to the phase instability of the uplink signal are grouped into: phase noise from the signal source itself (local oscillator), phase noise added from the electronic equipment at the transmitter side (internal noise), variations caused to the transmission channel due to atmospheric perturbations and phase noise added during frequency distribution [25].

The signal sources (local oscillators) for the ground systems in similar applications are based on maser technology with very low phase noise, which is insignificant to affect the operation of such systems [28]. Moreover, previous works have provided analytical models to describe the phase noise of imperfect oscillators and have introduced methods on how to compensate it [29,30].

Being an important aspect, solutions have already been investigated to guarantee phase stability in uplink array systems where internal noise at the ground stations is present [28]. This approach consists on installing sensors on the ground antennas to measure the phase stability and implementing closed loop circuits for the entire electronic pathways to correct imperfections.

Even though it is not the focus of this work, special attention is given to atmospheric perturbations. The signals being transmitted from the ground stations to the satellite suffer phase scintillation while propagating in the troposphere. If not dealt properly, phase scintillation can overpower the residual phase noise due to imperfect ground synchronization. In a similar application, it was shown that, such impairments can be compensated by introducing phase adjustments through complex multiplications in the transmission path of the ground antennas transmitting to a GEO satellite [27]. However, it is important to estimate the atmospheric perturbation as reliably as possible and avoid that the estimation is outdated when used for compensation. Mathematical models can be used to evaluate the impact of atmospheric phase scintillation [31]. Using an elevated layer model for the phase scintillation and assuming an atmospheric turbulence strength of 10^{-14} $m^{2/3}$, the standard deviation of the phase difference uncertainty between the signal paths from two widely separated ground stations amounts to a maximum of a thousandth of a radian, if the delay between channel estimation and phase pre-compensation does not exceed 10 ms. As will be seen later, such an instability is insignificant when compared to the standard deviation of the residual phase noise due to imperfect synchronization. Nevertheless, guaranteeing a time delay of 10 ms between channel observation and phase compensation is a challenging task. To avoid using a full feedback loop (which would require a time delay of about 300 ms), the downlink estimation technique has been investigated as a solution to reduce the observation time delay [32]. This technique consists on continuously transmitting a separate signal from the satellite to the ground to estimate the atmospheric perturbation.

Analogously to the analysis of timing alignment, without synchronization, the local oscillators of the ground stations in Fig. 1 would be free-running. Therefore, a frequency reference is introduced to synchronize the oscillators. However, considering that the reference is connected over long distance fiber links to the ground stations, phase noise is accumulated during the distribution. To cancel it out, the active phase noise compensation technique, shortly discussed in the Introduction, is implemented. Nevertheless, a residual phase mismatch will always be present between the ground stations and the reference source. In Fig. 1, the residual phase noise added during distribution from the reference to the ground stations is presented through the phase shifts $\xi_1(\tau)$, $\xi_2(\tau)$, ... and $\xi_N(\tau)$. As a consequence, the signals to be transmitted from the ground antennas will experience slightly different phase perturbations. In Section 4, the limitation that the residual phase uncertainties bring in the performance of a MIMO feeder link is analyzed.

2.3 | Independent time and phase synchronization

As implied by Fig. 1, time and phase synchronization are considered independent of each-other. There are different approaches to guarantee the independence of the synchronization techniques over optical fiber. The classical solution would be to use two separate optical fibers links and transmit the time/frequency signals independently[33,34]. With the intention of saving resources, another solution would be a joint time and frequency distribution technique[35]. It consist on adding the time signal as a violation pattern over the falling edges of a square wave used as the frequency reference. The violation does not affect the rising edges of the square wave, but only the falling ones. Therefore, the phase alignment segment is not affected and time alignment is guaranteed. Taking this into account, time and phase synchronization are treated separately for the rest of the paper.

3 | IMPACT OF IMPERFECT TIME SYNCHRONIZATION

The residual time difference due to imperfect time distribution limits the signal bandwidth that can be supported by the MIMO system. In this section, a mathematical model that governs the relation between the achievable bandwidth and the time misalignment is calculated. For a better understanding of the math involved, the reader is advised to refer to an earlier work on which this paper is based on, Mollaymeri et al. (2022)[36]. The impulse response of the NxN MIMO channel, considering the time mismatches due to imperfect time distribution between the ground stations and the time reference, is modeled as follows:

$$\mathbf{H}(t;\tau) = \sum_{i=1}^{N} \tilde{\mathbf{H}}_{\mathbf{0},\mathbf{i}}(\tau) \cdot \delta\left\{t - \varepsilon_i(\tau)\right\} \tag{1}$$

where, $i = 1, 2, ..., N$, f is the operating frequency and $\tilde{\mathbf{H}}_{\mathbf{0},\mathbf{i}}(\tau)$ is the channel matrix with all the channel coefficients being equal to 0 except in the i-th column. On the other hand, the transfer function is equal to:

$$\mathbf{T}(f;\tau) = \sum_{i=1}^{N} E_{\varepsilon_i(\tau)}\left\{\tilde{\mathbf{H}}_{\mathbf{0},\mathbf{i}}(\tau) \cdot e^{-j2\pi f \varepsilon_i(\tau)}\right\} \tag{2}$$

With the assumption that the $\varepsilon_i(\tau)$ elements are identically distributed Gaussian random variables with zero mean and standard deviation σ_ε, the transfer function can be represented in terms of a single variable, namely $\varepsilon(\tau)$:

$$\mathbf{T}(f;\tau) = \tilde{\mathbf{H}}(\tau) \cdot E_{\varepsilon(\tau)}\left\{e^{-j2\pi f \varepsilon(\tau)}\right\} = \tilde{\mathbf{H}}(\tau) \cdot e^{-2\pi^2 f^2 \sigma_\varepsilon^2} \tag{3}$$

where, f is the operating frequency and $\tilde{\mathbf{H}}(\tau)$ is the channel matrix with the channel coefficients. As mentioned beforehand, the goal is to better understand the effect of $\varepsilon(\tau)$ on the supported MIMO channel bandwidth (B). First, we can derive the 3-dB cut-off frequency (f_{3dB}) using the expression below:

$$|\mathbf{T}(f_{3dB};\tau)|^2 = \frac{1}{2} \cdot |\mathbf{T}(0;\tau)|^2 = \frac{1}{2} \cdot \left|\tilde{\mathbf{H}}(\tau)\right|^2 \tag{4}$$

The outcome of solving (4) demonstrates that the bandwidth is equal to:

$$B = 2 \cdot f_{3dB} = 2 \cdot \frac{\sqrt{\ln(2)}}{2\pi\sigma_\varepsilon} \approx \frac{0.265}{\sigma_\varepsilon} \tag{5}$$

In Fig. 2, the relation of the achievable bandwidth to the standard deviation of $\varepsilon(\tau)$ is shown in logarithmic scale. Evidently, the bandwidth increases when σ_ε becomes smaller. For a better understanding, some examples for the standard deviation and the corresponding bandwidth are given in Table 1. The feeder links of HTS systems need to support multiple carriers simultaneously. Operation in the Q/V band offers a total uplink bandwidth of 5 GHz with carriers which can reach up to 1 GHz each[37]. A bandwidth of 500 MHz or 1 GHz would, for example, necessitate a standard deviation for $\varepsilon(\tau)$ not exceeding 530 ps or 265 ps respectively. Based on the uncertainty figures of conventional methods such as GPS (10 ns to 20 ns), it is necessary to utilize better performing time distribution techniques that support the demands of MIMO feeder links. The ability of the time distribution via optical fiber approach to guarantee the desired stability has been verified in an experimental setup presented in Section 5.

4 | IMPACT OF IMPERFECT PHASE SYNCHRONIZATION

To achieve optimum operation, one needs to continuously estimate the channel coefficients of the MIMO feeder link and adapt the precoding matrix accordingly[10]. However, the estimation accuracy is immensely disturbed by the phase mismatches between the ground antennas. In this section, a mathematical model that relates the limitation of the channel estimation performance to the residual phase uncertainties is introduced.

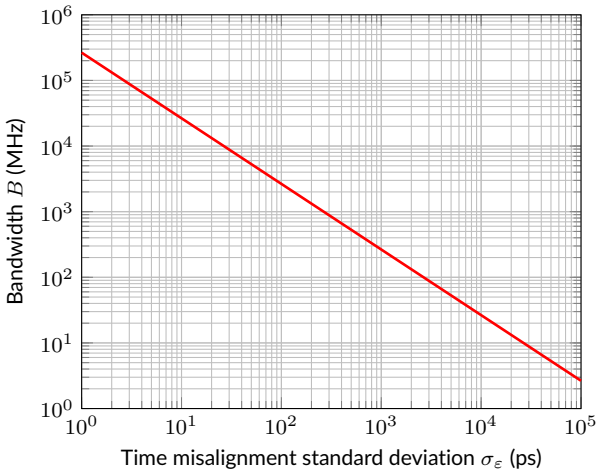

Figure 2 The achievable signal bandwidth in a NxN MIMO feeder link under the presence of time misalignment.

Table 1 Achievable bandwidth given the time misalignment standard deviation.

Standard Deviation σ_ε (ns)	**Bandwidth B (GHz)**
0.265	1
0.53	0.5
10	0.0265
20	0.0133

In Fig. 1, $\phi_n(\tau)$ represents the phase shift for the n-th ground antenna. For ease of explanation, we assume that the reference block is placed at GW_1 and is connected over the fiber to the other gateways, which means that $\xi_1(\tau)$ is equal to 0. Considering that the local oscillators are assumed to have a very low phase noise such that the perturbation from the oscillators can be neglected, after achieving synchronization, the following holds: $\phi_j(\tau) = \phi_1(\tau) + \xi_j(\tau)$, where $j = 2, .., N$. The $\xi_j(\tau)$ elements are assumed to be independent and identically distributed Gaussian random variables with zero mean and standard deviation σ_{ξ_j}. In the model considered, the precoder coefficients are computed from an estimation of the MIMO channel and not the exact one [10]. The imperfect channel state information (CSI) for the NxN MIMO feeder link can be represented in terms of the elements $\xi_j(\tau)$ as follows:

$$\tilde{\mathbf{H}}(\tau) = \hat{\mathbf{H}}(\tau) \cdot \begin{bmatrix} e^{j\phi_1(\tau)} & 0 & \cdot & 0 \\ 0 & e^{j\phi_2(\tau)} & \cdot & 0 \\ \cdot & \cdot & \cdot & \cdot \\ 0 & 0 & \cdot & e^{j\phi_N(\tau)} \end{bmatrix} = e^{j\phi_1(\tau)} \cdot \hat{\mathbf{H}}(\tau) \cdot \begin{bmatrix} 1 & 0 & \cdot & 0 \\ 0 & e^{j\xi_2(\tau)} & \cdot & 0 \\ \cdot & \cdot & \cdot & \cdot \\ 0 & 0 & \cdot & e^{j\xi_N(\tau)} \end{bmatrix} \tag{6}$$

where, $\hat{\mathbf{H}}(\tau)$ is the estimate of the effective channel. Since the phase component $e^{j\phi_1(\tau)}$ on the right hand side of (6) is applied to all the channel coefficients of $\hat{\mathbf{H}}(\tau)$, only the variables $\xi_j(\tau)$ affect the CSI quality. The probability distribution function of $\xi_j(\tau)$ is given as:

$$f_{\xi_j}\{\xi_j(\tau)\} = \frac{1}{\sqrt{2\pi\sigma^2_{\xi_j}}} \cdot e^{-\frac{\xi_j^2(\tau)}{2\sigma^2_{\xi_j}}} \tag{7}$$

The CINR is considered to asses the effect of the phase noise uncertainties on the performance of an NxN MIMO feeder link. If optimum distance between the ground stations and no rain attenuation are assumed, the CINR values of the data streams from the ground antennas to the satellite in Fig. 1 would be equal. The CINR for the first data stream is calculated as:

$$\rho_1(\tau) = \frac{\left|\tilde{\mathbf{H}}(\tau)\mathbf{b}_{\hat{\mathbf{H}},1}(\tau)\right|^2}{\sum_{j=2}^{N}\left\{\left|\tilde{\mathbf{H}}(\tau)\mathbf{b}_{\hat{\mathbf{H}},j}(\tau)\right|^2\right\} + 2\sigma_\eta^2} \tag{8}$$

where, $\mathbf{b}_{\hat{\mathbf{H}},i}(\tau)$ is the precoding vector for the i-th user ($i = 1, 2...N$) and σ_η is the standard deviation of the noise added to the data stream modeled as Gaussian distribution.

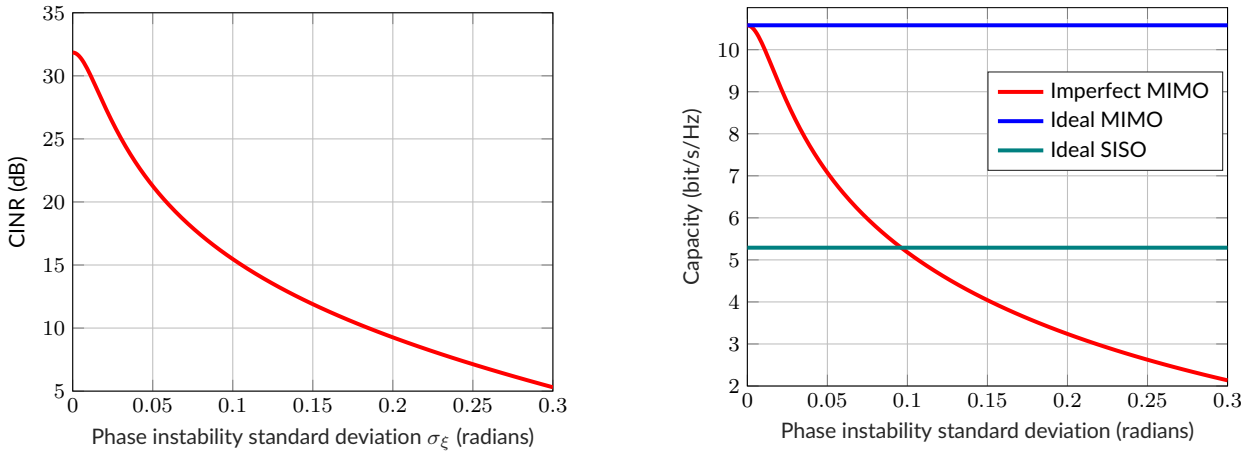

Figure 3 CINR (left) and capacity (right) as a function of the standard deviation of the phase instability (σ_ξ) for a 2x2 MIMO feeder link.

To better understand the effect that the phase uncertainty has on the achievable CINR we look at an example scenario for a 2x2 MIMO feeder link. In such a case, only $\xi_2(\tau)$ affects the CSI according to (6). We then analyze the risk of a link outage due to a large value of $\xi_2(\tau)$. The CINR is calculated for the value $\xi_2^{0.1}$, exceeded by only 0.1 % of the realizations of $\xi_2(\tau)$. Based on (7), it can be shown that:

$$\xi_2^{0.1} = \sigma_{\xi_2} \cdot Q^{-1}\left(\frac{0.1}{200}\right) \tag{9}$$

where, $Q(.)$ stands for the Q-function. The calculation of the minimum CINR value guaranteed for 99.9 % of the realizations (referred to as just CINR for the remaining of the paper) comes as an extension of previous works on MIMO feeder links [10].

The resulting CINR values for the 2x2 MIMO feeder link are illustrated in Fig. 3 (left) for standard deviation values varying from 0 to 0.3 radians. According to the results, there would be a considerable performance drop for even a small amount of phase uncertainty present. If, for example, there is a constraint that the CINR performance should not drop by more than 1 dB, the phase instability standard deviation should be below 0.008 radians. Therefore, it is important to keep the residual phase noise due to imperfect phase synchronization of the ground stations to a minimum.

The counterpart scenario of the MIMO setup is the benchmark single-input single-output (SISO) application. Phase synchronization between the ground stations of a SISO system is unnecessary because its links are independent. Therefore, the question rises whether there is an advantage using MIMO feeder links considering the effect of phase instability between the ground stations. Moreover, if such an advantage exists, at what level should the phase instability be kept so that better performance than SISO is guaranteed? To answer this question, the capacity of the MIMO feeder link was calculated, based on the CINR values for different phase instability standard deviation. The results are plotted in Fig. 3 (right) together with the capacity of the ideal MIMO (without phase instability) and SISO scenarios. In a SISO feeder link system there are M antenna sites separated by hundreds of kilometers providing M spatially separated links. In the case of a 2x2 MIMO feeder link system, each antenna site consists of 2 antennas up to 50 kilometers apart, doubling the capacity of each feeder link if the satellite is equipped with two spatially separated antennas. As a result, $M/2$ antenna sites separated by hundreds of kilometers are, in theory, able to provide the same feeder link capacity as a SISO feeder link system with M antenna sites [10]. However, the presence of phase uncertainty due to the imperfect phase synchronization between ground stations in a MIMO feeder link, does not allow to guarantee this advantage fully. To assure a better performance, it is important that the capacity of MIMO feeder links remains sufficiently higher than for SISO feeder links. According to Fig. 3 (right), this is the case if the phase uncertainty remains below 0.05 radians, where it can be guaranteed that the MIMO capacity is at least 1.3 times larger than for SISO.

In section 5.2, a phase synchronization technique based on active phase noise compensation is introduced. The uncertainty numbers from this approach are applied to formula (8) and the results are analyzed.

5 | PRACTICAL VERIFICATION OF SYNCHRONIZATION SOLUTIONS

In this section, the distribution of time and phase via optical fiber is discussed. Experimental trials were carried to test time synchronization over a few tens of kilometres. On the other hand, an approach for very stable frequency distribution over fiber in antenna arrays is introduced.

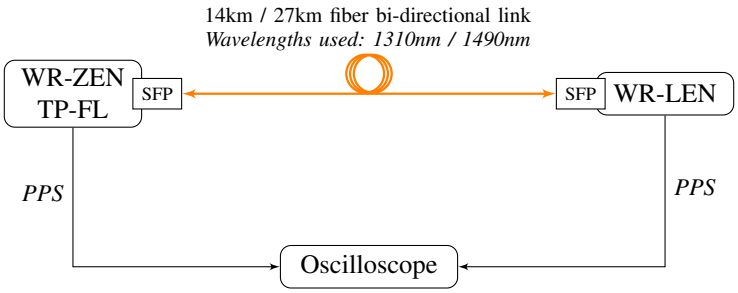

Figure 4 Architecture of the White Rabbit experiment for time distribution.

5.1 | White Rabbit standard for time distribution

A commercial off-the-shelf solution was chosen to test the time distribution over optical fiber. The White Rabbit standard has been developed by the European Organization for Nuclear Research (CERN) to provide time synchronization in distributed systems. It has since been used for different applications, including the synchronization of antenna arrays[38]. The designers of the White Rabbit standard suggest that the solution is able to support picoseconds precision of synchronization[39]. Moreover, previous works have shown that it can cover distances of hundreds of kilometers[40,41]. In a practical scenario, for example, the ground stations for a 2x2 MIMO feeder link are placed between 30 km to 50 km apart. Therefore, based on the properties mentioned above, the White Rabbit devices are a suitable candidate to support the bandwidth requirements discussed in Section 3.

5.1.1 | Experimental setup

A simplified schematic representation of the architecture of the experiment for testing the time synchronization between two White Rabbit devices separated by a few kilometers is illustrated in Fig. 4. One of the White Rabbit devices, namely WR-ZEN TP-FL, acts as the master and the other one, WR-LEN, acts as a slave. This means that once connected over the fiber, the WR-LEN will have its time synchronized to the master. In the context of the MIMO feeder link shown in Fig. 4, the White Rabbit master device would act as the time reference block and a White Rabbit slave device would be placed at each ground station. The setup was tested by connecting the White Rabbit devices with a 14298 m long fiber (referred to as 14 km for the remaining of the paper) and then with a 27406 m fiber (referred to as 27 km for the remaining of the paper). The White Rabbit devices are connected to the fiber using bi-directional small form-factor pluggable transceivers (SFP) with different wavelengths for transmission and reception, namely 1310 nm for the transmission from the master to the slave and 1490 nm for the other way around. The single bi-directional fiber connection is the recommended configuration by CERN to achieve the smallest possible delay asymmetry[41,40].

We are interested in studying the time misalignment between the White Rabbit devices. To do this, we calculated their pulse-per-second (PPS) offset. The PPS signals are one of the outputs one can get from such devices. The signal has a short pulse that accurately repeats once per second. Using an oscilloscope, we were able to capture the rising edges of the corresponding PPS pulses. We used the oscilloscope RTO 1044 from Rohde & Schwarz for our experiment, setting its vertical resolution and sampling rate to the maximum, 16-bit and 20 GSa/s respectively. Afterwards, MATLAB was used to acquire the rising edges from the oscilloscope and to calculate the time difference between their 50 % levels. The reader is advised to refer to Mollaymeri et al. (2022)[36] for a better understanding of the procedure for calculating the PPS offset.

5.1.2 | PPS-offset values from the experiment

The PPS offset was calculated every second for 3 hours. Eventually, we acquired 10800 PPS offset values from the setup with the 14 km fiber and the 27 km one. Finding which distribution fits the PPS offset between the two White Rabbit devices would help in calculating the variance and, as a result, the achievable bandwidth for each system, based on the model of Section 3. To achieve this, we calculated the histograms of the two batches of PPS offset values and tried to fit Gaussian distributions to them. In the technique we implemented for the fitting, the estimated value of the standard deviation is calculated as the square root of the unbiased estimate of the variance, using maximum likelihood estimation. The histograms for the 14 km and 27 km fiber connections and their fitted Gaussian distributions (colored in red) are illustrated in Fig. 5 respectively.

Due to limitations from the measuring equipment and the MATLAB acquisition procedure, we were met with the known long tails problem for the histogram of the 14 km fiber setup. To capture the rising edges of the PPS pulse, we had to limit the acquisition time to 1 ns. Using the maximum sampling rate supported by the oscilloscope (20 GSa/s), we were able to acquire 2000 samples (involving an interpolation of factor 100). This allowed for a time resolution of 0.5 ps. However, the oscilloscope is able to zoom in down to only 10 mV for the amplitude. Considering the vertical resolution of 16-bit that the device supports, the amplitude was divided into bins of 152.6 nV. Therefore, there was a noticeable difference

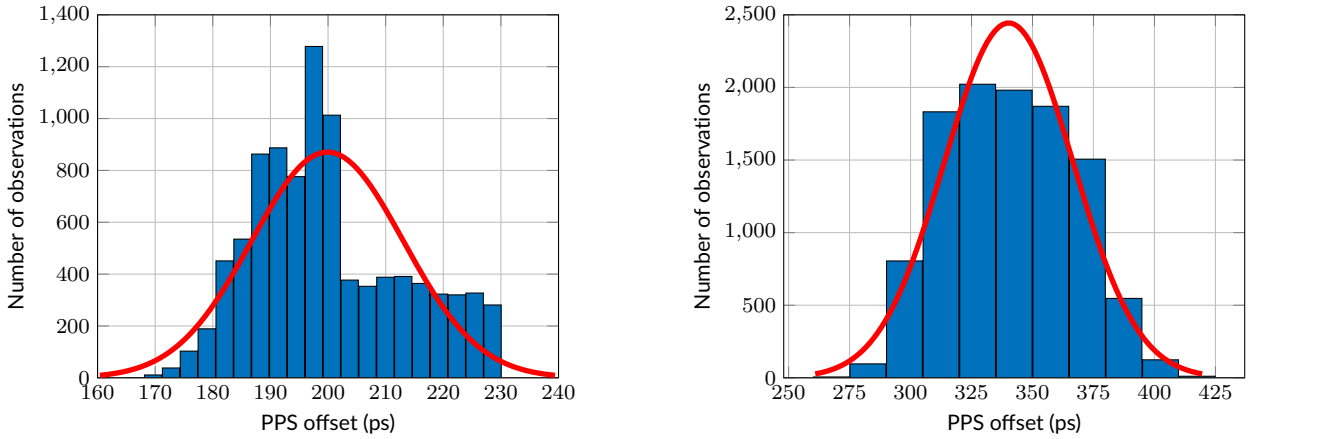

Figure 5 Histogram and the fitted Gaussian distribution of the PPS offset for the scenario with the 14 km fiber (left) and the 27 km fiber (right).

between the granularity supported for the amplitude and the one for the time. As a consequence, several PPS values, corresponding to different sampling time instances, were rounded within one amplitude bin. This affected the procedure for finding the 50 % level of the PPS rising edges. To find these levels, we had to take a time average between the samples of the corresponding amplitude bin. In the case of the 14 km fiber setup, the PPS values were too small and this problem was highly pronounced. Measuring the PPS offset values lead in a longer tail for the upper part of the histogram. To deal with it, a section of the long tail was removed when fitting the normal distribution.

On the other hand, as expected, the PPS offset values for the 27 km fiber setup are higher when compared to the 14 km one, since a longer distance needs to be covered for the time distribution. As a consequence, in this application, the long tail problem is not persistent and the histogram is already quite similar to a Gaussian shape, as noticed in Fig. 5 (right).

The plots demonstrate that the measured PPS offsets between the two White Rabbit devices have a non-zero mean. It comes as a consequence of the residual calibration error. The error is bigger for the 27 km fiber model, since the calibration has to compensate for the longer transmission path. Nevertheless, in a practical scenario, measuring it is a straight forward procedure and one can compensate for it by applying accordingly a controlled delay to the paths. Therefore, a zero mean can be reasonably assumed for the timing imperfection. Hence, it is not necessary to consider it in the calculation of the MIMO feeder link bandwidth.

5.1.3 | Supported bandwidth

Based on the histograms in Fig. 5 and the overlaid Gaussian distributions, we are able to infer their distribution characteristics. The fitted Gaussian curves have a standard deviation of 13.17 ps for the 14 km fiber scenario and 26.44 ps for the 27 km fiber scenario. Knowing the values for the standard deviation of the PPS offset for the White Rabbit architecture explained in Section 5, we are able to calculate the corresponding channel bandwidths, if we were to implement the White Rabbit architecture for the MIMO feeder link in Section 3. Table 2 shows the resulting bandwidths, calculated by replacing the standard deviation values for the 14 km fiber and 27 km fiber scenarios in (5).

Table 2 Supported bandwidth for White Rabbit experiments with 14 km and 27 km fiber.

Distance (km)	Bandwidth (GHz)
14	20.1
27	10

The results in Table 2 and the analysis in Section 3 prove that the optical fiber time distribution approach implemented with the White Rabbit standard is able to support the necessary bandwidth for a single carrier in MIMO feeder links. Comparing the values of the achievable bandwidths for the 14 km and 27 km architectures, would lead to the conclusion that distributing the time over a distance that is twice longer leads to a reduction of the bandwidth by a factor 2. Previous works on White Rabbit architectures have shown that chromatic dispersion is the main stability limiting factor[41]. Results show that the effect of chromatic dispersion on the achievable stability is negligible for the considered distances, but it would be considerable for longer distances. As such, further experiments with longer fibers are needed to better understand the relation between the length of the fiber and the achievable bandwidth under the presence of chromatic dispersion. Nevertheless, a typical separation for ground stations in MIMO feeder links oscillates between 30 km and 50 km, which is comparable to the lengths considered in this work. Considering that the supported bandwidth for the 27 km fiber is at least 10 times higher than the necessary bandwidth per carrier in a MIMO feeder link (500 MHz

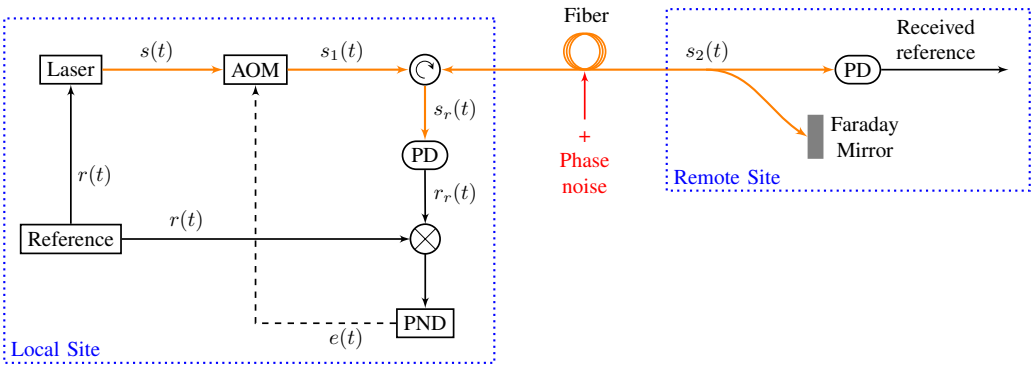

Figure 6 Architecture of the active phase noise compensation technique.

to 1 GHz), the results from the White Rabbit experiment suggest that the bandwidth requirements can be comfortably supported even for a fiber length of 50 km.

5.2 | Phase synchronization in the Square Kilometre Array project

The Square Kilometre Array project is an international effort to build the world-leading radio telescope. Among others, it consists on interconnecting about 200 antennas separated by tens of kilometres. For an optimum operation, it is of crucial importance to align in phase the distributed ground systems. The work of Schediwy et al. (2019)[22] proposes a phase synchronization technique, based on active compensation of the phase noise, that aims to fulfill the stringent requirements of the Square Kilometre Array project. Our goal is to investigate the ability of this approach to support the demands of a MIMO feeder link application. To this end, we analyze the functionality of such a technique through a simplified representation. We encourage the reader to refer to the before-mentioned work for a detailed explanation on the tested architecture.

In Fig. 6, the simplified version of the active phase noise compensation technique via optical fiber frequency distribution is illustrated. The intention of the setup is to transfer the reference signal $r(t)$ over the fiber from a local site to a remote one, while dealing with the accumulated phase noise. First, the reference signal modulates the output of a laser to generate the optical signal $s(t)$. Thereafter, $s(t)$ is frequency shifted by an acousto-optic modulator (AOM) generating the signal $s_1(t)$ as an output, which is transmitted over the fiber to the remote site. During the transmission over the fiber, $s_1(t)$ accumulates phase noise due to temperature drifts and hardware imperfections. Therefore, the received signal at the remote site is denoted with $s_2(t)$. This optical signal is split and part of it is detected by a photo-detector (PD), which extracts the reference. The other part of the signal is reflected back to the local site using a Faraday mirror. The signal $s_2(t)$ passes again through the fiber and, consequently, more phase noise is accumulated. At the local site an optical circulator directs the incoming optical signal $s_r(t)$ (with the added phase noise) to a photo-detector, which extracts the imperfect reference $r_r(t)$. The local reference $r(t)$ is mixed with the noisy reference $r_r(t)$ and the resulting signal is sensed by a phase noise detector (PND). The phase noise detector extracts the phase difference between the two references and generates an error signal $e(t)$ which controls the frequency shift applied to the optical signal $s(t)$ by the acousto-optic modulator. As a result, a feedback loop is generated to continuously cancel out the phase noise that is added during the transmission over the fiber.

The architecture tested by the authors of Schediwy et al. (2019)[22] mixes two 40 MHz signals at the local site. One of the signals is a down-converted version of the actual reference, while the other one is a down-converted noisy reference which has been transmitted over a 166 km fiber to and from the remote site. Even though the authors of this work guarantee a high performance, there will be residual phase uncertainty left. To calculate it, they measured the phase drift in intervals of 10 minutes for a period of 15 hours. According to their findings, the standard deviation of the residual phase instability was 14 μrad.

MIMO feeder links operate at a frequency of around 50 GHz. Therefore, the instability is expected to increase by a factor 1250 (50 GHz divided by 40 MHz) when up-converting the reference signal. As a consequence, for the scenario of interest, the standard deviation of the phase uncertainty would increase to 0.0175 rad. As mentioned earlier, the distance for which the phase synchronization was tested for was 166 km. For such long distances, the effect of chromatic dispersion is highly pronounced, influencing also the phase instability. Furthermore, there is a linear relation between chromatic dispersion and the length of the fiber[41]. Therefore, in the worst case scenario, it can be assumed that the standard deviation of the phase instability reduces linearly with the fiber length. Hence, for a maximum distance of 50 km between the ground stations in a MIMO feeder link, we can consider a factor 3.32 (166 km divided by 50 km) reduction on the standard deviation of the phase instability. As a result, the standard deviation would be about 0.0053 rad. This value is below the limit of 0.008 rad discussed in Section 4 for a 1 dB CINR reduction. Moreover, it is about a factor 10 lower than the limit that would guarantee a higher capacity for a MIMO link (using two ground stations) compared to a SISO link.

6 | CONCLUSIONS

In this paper, mathematical models that describe the behavior of an NxN MIMO feeder link under the presence of time and phase misalignment due to imperfect synchronization were presented. The theoretical analysis indicates that MIMO feeder links have extensive requirements with respect to the channel bandwidth and link outage.

Through an experimental verification, it was demonstrated that time distribution over optical fiber would support the immense bandwidth demands of NxN MIMO feeder links in the order of several GHz. The experiment trials indicate that, these numbers can be achieved even through commercially available solutions of time distribution such as the White Rabbit standard. Furthermore, results from the phase synchronization technique tested for the Square Kilometre Array support the requirements of MIMO feeder links in terms of achievable CINR values. The approach based on phase distribution over optical fiber demonstrated the superiority of the later technique even for phase synchronization. The proposed techniques are especially advantageous because the existing fiber infrastructure might be considered to guarantee time and phase distribution.

For the future, it is of interest to take this study in further research directions. First, considering the promising time synchronization results with the White Rabbit setup, longer distances could be investigated. Another goal is to extend the developed testbed with the phase synchronization approach discussed in this work. This extension will enable a complete experimental verification of a MIMO feeder link architecture. Additionally, considering the importance of time and phase alignment in multiple-gateway systems, the relevance of the results presented in this work is not limited to MIMO feeder links.

References

1. Gharanjik A, MR BS, Arapoglou PD, Ottersten B. Multiple gateway transmit diversity in Q/V band feeder links. *IEEE Transactions on Communications* 2014; 63(3): 916–926.

2. Fenech H, Amos S, Tomatis A, Soumpholphakdy V. High throughput satellite systems: An analytical approach. *IEEE Transactions on Aerospace and Electronic Systems* 2015; 51(1): 192–202.

3. Joroughi V, Vázquez MÁ, Pérez-Neira AI. Precoding in multigateway multibeam satellite systems. *IEEE Transactions on Wireless Communications* 2016; 15(7): 4944–4956.

4. Christopoulos D, Pennanen H, Chatzinotas S, Ottersten B. Multicast multigroup precoding for frame-based multi-gateway satellite communications. In: *2016 8th Advanced Satellite Multimedia Systems Conference and the 14th Signal Processing for Space Communications Workshop (ASMS/SPSC)*. IEEE. ; 2016: 1–6.

5. Piazza R, MR BS, Ottersten B. Multi-gateway data predistortion for non-linear satellite channels. *IEEE Transactions on Communications* 2015; 63(10): 3789–3802.

6. Zhu Y, Hofmann CA, Knopp A. Performance Optimization for Multi-Gateway NOMA-Beamforming in Multi-Beam SATCOM. In: *ICC 2021-IEEE International Conference on Communications*. IEEE. ; 2021: 1–6.

7. Kyrgiazos A, Evans B, Thompson P. Smart gateways designs with time switched feeders and beam hopping user links. In: *2016 8th Advanced Satellite Multimedia Systems Conference and the 14th Signal Processing for Space Communications Workshop (ASMS/SPSC)*. IEEE. ; 2016: 1–6.

8. Tani S, Uchida S, Okamura A. Overlapping clustering for beam-hopping systems. In: *36th International Communications Satellite Systems Conference (ICSSC 2018)*. IET; 2018.

9. Shah HM, Mishra P, Mishra N, Jain P, Saiyed MA, Banik A. An onboard digital transparent processor for a multi-beam satellite. In: *2015 2nd International Conference on Signal Processing and Integrated Networks (SPIN)*. IEEE. ; 2015: 366–371.

10. Delamotte T, Knopp A. Smart diversity through MIMO satellite Q/V-band feeder links. *IEEE Transactions on Aerospace and Electronic Systems* 2019; 56(1): 285–300.

11. Beidas BF. High-Capacity, Weather-Resilient MIMO Feeder Links in Multibeam Satellite Systems. *IEEE Transactions on Communications* 2022.

12. Guidotti A, Sacchi C, Vanelli-Coralli A. Feeder Link Precoding for Future Broadcasting Services: Architecture and Performance. *IEEE Transactions on Aerospace and Electronic Systems* 2022.

13. NOAA . *Official U.S. government information about the global positioning system (GPS) and related topics: Timing application*. https://www.gps.gov/applications/timing; 2022. Accessed November 14, 2022.

14. Lewandowski W, Azoubib J, Klepczynski WJ. GPS: Primary tool for time transfer. *Proceedings of the IEEE* 1999; 87(1): 163–172.

15. Lombardi MA, Nelson LM, Novick AN, Zhang VS. Time and frequency measurements using the global positioning system. *Cal Lab: International Journal of Metrology* 2001; 8(3): 26–33.

16. Cacciapuoti L, Salomon C. Space clocks and fundamental tests: The ACES experiment. *The European Physical Journal Special Topics* 2009; 172(1): 57–68.

17. Śliwczyński Ł, Krehlik P, Buczek Ł, Lipiński M. Active propagation delay stabilization for fiber-optic frequency distribution using controlled electronic delay lines. *IEEE Transactions on Instrumentation and Measurement* 2010; 60(4): 1480–1488.

18. Singh V, Prabhakara A, Zhang D, Yağan O, Kumar S. A community-driven approach to democratize access to satellite ground stations. *GetMobile: Mobile Computing and Communications* 2022; 26(1): 35–38.

19. Lopez O, Kanj A, Pottie PE, et al. Simultaneous remote transfer of accurate timing and optical frequency over a public fiber network. *Applied Physics B* 2013; 110(1): 3–6.

20. Krehlik P, Śliwczyński Ł, Buczek Ł, Kołodziej J, Lipiński M. ELSTAB—Fiber-optic time and frequency distribution technology: A general characterization and fundamental limits. *IEEE transactions on ultrasonics, ferroelectrics, and frequency control* 2015; 63(7): 993–1004.

21. Hsu MT, He Y, Shaddock DA, Warrington RB, Gray MB. All-digital radio-frequency signal distribution via optical fibers. *IEEE Photonics Technology Letters* 2012; 24(12): 1015–1017.

22. Schediwy S, Gozzard D, Gravestock C, et al. The mid-frequency square kilometre array phase synchronisation system. *Publications of the Astronomical Society of Australia* 2019; 36.

23. Wang X, Wei W, Dong Y. Enhanced frequency stability over fiber link with improved phase discrimination scheme. *IEEE Access* 2019; 7: 171405–171410.

24. Liu C, Zhou S, Shang J, et al. Stabilized radio frequency transfer via 100 km urban optical fiber link using passive compensation method. *IEEE Access* 2019; 7: 97487–97491.

25. Davarian F. Uplink arraying for solar system radar and radio science. *Proceedings of the IEEE* 2011; 99(5): 783–793.

26. Delamotte T. *MIMO feeder links for very high throughput satellite systems*. PhD thesis. Universitätsbibliothek der Universität der Bundeswehr München, ; 2019.

27. Martin GP, Minear KM. System and method for widely-spaced coherent transmit arraying using a remote receiver.; 2019. US Patent 10,270,506.

28. Martin P, Minear K, Geldzahler B, Soloff J. Large reflector uplink arraying. In: *SpaceOps 2010 Conference Delivering on the Dream Hosted by NASA Marshall Space Flight Center and Organized by AIAA*. ; 2010: 2175.

29. Piemontese A, Colavolpe G, Eriksson T. A New Analytical Model of Phase Noise in Communication Systems. In: IEEE. ; 2022: 926–931.

30. Colavolpe G, Foggi T, Forestieri E, Secondini M. Impact of phase noise and compensation techniques in coherent optical systems. *Journal of Lightwave Technology* 2011; 29(18): 2790–2800.

31. Wheelon AD. *Electromagnetic scintillation: volume 2, weak scattering*. Cambridge University Press . 2003.

32. Martin GP, Minear K. Systems and methods for compensating for transmission phasing errors in a communications system using a receive signal.; 2011. US Patent 7,970,365.

33. Hendre A. Precise frequency and time transfer for the square kilometer array. *Sensors and Electronic Instrumentation Advances* 2020; 2: 204.

34. Śliwczyński Ł, Krehlik P, Lipiński M. Optical fibers in time and frequency transfer. *Measurement Science and Technology* 2010; 21(7): 075302.

35. Krehlik P, Sliwczynski Ł, Buczek Ł, Lipínski M. Fiber-optic joint time and frequency transfer with active stabilization of the propagation delay. *IEEE Transactions on instrumentation and measurement* 2012; 61(10): 2844–2851.

36. Mollaymeri E, Delamotte T, Knopp A. Timing Alignment of Distributed Gateways: Theoretical Analysis and Experimental Demonstration. In: IEEE. ; 2022: 1–8.

37. Mody A, Gonzalez E. An operator's view: The medium-term feasibility of an optical feeder link for VHTS. In: *2017 IEEE International Conference on Space Optical Systems and Applications (ICSOS)*. IEEE. ; 2017: 278–285.

38. Jiménez-López M, Torres-González F, Gutiérrez-Rivas JL, Rodríguez-Álvarez M, Díaz J. A fully programmable white-rabbit node for the SKA telescope PPS distribution system. *IEEE Transactions on Instrumentation and Measurement* 2018; 68(2): 632–641.

39. Lipinski R. *The White Rabbit Project*. https://white-rabbit.web.cern.ch; 2022. Accessed November 15, 2022.

40. Dierikx EF, Wallin AE, Fordell T, et al. White rabbit precision time protocol on long-distance fiber links. *IEEE transactions on ultrasonics, ferroelectrics, and frequency control* 2016; 63(7): 945–952.

41. Kaur N. *Long range time transfer over optical fiber links and cross-comparison with satellite based methods*. PhD thesis. SYRTE, Observatoire de Paris, ; 2018.

42. Storek KU, Schwarz RT, Knopp A. Multi-satellite multi-user MIMO precoding: Testbed and field trial. In: *ICC 2020-2020 IEEE International Conference on Communications (ICC)*. IEEE. ; 2020: 1–7.

AUTHOR BIOGRAPHY

Eriserdi Mollaymeri received his Bachelor's degree in Electronic Engineerig from the Polythecnic University of Tirana, Albania, in 2015. He followed the Master's studies for Communications and Multimedia Engineering at the Friedrich Alexander University in Erlangen, Germany and graduated in 2019. Since 2020, he has been a Research Fellow with the Department of Electrical Engineering and Information Technology at the University of the Bundeswehr in Munich, Germany. His research interests include satellite communications, digital signal processing and MIMO.

Thomas Delamotte received the master's degree in communications and network engineering from the National Polytechnic Institute of Toulouse, Toulouse, France, in 2009, and the Ph.D. degree (summa cum laude) in communications engineering from the Bundeswehr University Munich, Munich, Germany, in 2019. He was a Research Fellow with the Department of Electrical Engineering and Information Technology, Bundeswehr University Munich. Since 2016, he has been coordinating the Research Group Digital Satellite Payloads and Satellite Monitoring from the Chair of signal processing with the same university. He is currently engaged in several national and international research projects focusing on the application of advanced signal processing techniques and waveform designs for next-generation high-throughput satellite systems.

Andreas Knopp received the Ph.D. degree (Hons.) in radio communications from Bundeswehr University Munich, Munich, Germany, in 2008 Since 2014, he has been a Full Professor of satellite communications and holds the Chair of signal processing with Bundeswehr University Munich, where he is also a spokesman for the Interdisciplinary SPACE Research Center on space technologies. He is also a Visiting Professor with Naval Postgraduate School, Monterey, CA, USA, and Co-Founder of several start-up companies implementing his research. He has coauthored more than 120 scientific publications and six patents. His research interests include satellite network integration and waveform design for 6G, digital satellite payloads, secure/antijam communications, and low-power mMTC.

How to cite this article: E. Mollaymeri, T. Delamotte and A. Knopp (2022), Time and Phase Alignment of Distributed Gateways: Theoretical analysis and Experimental Demonstration., , .